An Investigation of Rigid p -Methylterphenyl Thiol Self-Assembled Monolayers on Au(111) Using Reflection−Absorption Infrared Spectroscopy and Scanning Tunneling Microscopy

ARTICLE *in* THE JOURNAL OF PHYSICAL CHEMISTRY B · OCTOBER 2001

Impact Factor: 3.3 · DOI: 10.1021/jp012123r

2 AUTHORS, INCLUDING:

Simon J. Garrett
California State University, Northridge
30 PUBLICATIONS **417** CITATIONS

SEE PROFILE

An Investigation of Rigid *p*-Methylterphenyl Thiol Self-Assembled Monolayers on Au(111) Using Reflection−Absorption Infrared Spectroscopy and Scanning Tunneling Microscopy

Lili Duan and Simon J. Garrett*

Department of Chemistry, Michigan State University, East Lansing, Michigan 48824

Received: June 5, 2001; In Final Form: July 23, 2001

We have prepared and characterized self-assembled monolayers (SAMs) of rigid *p*-methylterphenyl thiol (MTPT) on Au(111). According to ellipsometry and reflection−absorption infrared spectroscopy (RAIRS), MTPT forms densely packed monolayers on gold with the molecular axes slightly tilted away from the surface normal (∼17°). At room temperature, monatomically high islands are observed by scanning tunneling microscopy (STM) instead of the typical monatomically deep holes characteristic of alkanethiol films. Molecular resolution images of the MTPT monolayer reveal a $(\sqrt{3}\times\sqrt{3})$R30°-like packing with slightly larger lattice vectors ($a = 5.3 \pm 0.3$ Å, $b = 5.3 \pm 0.4$ Å, $\gamma = 60° \pm 2°$) than those of typical alkanethiol monolayers. This is probably due to the mismatch between the lowest energy packing configuration of the terphenyl monolayer (similar to that of crystalline terphenyl solid) and that of the underlying $(\sqrt{3}\times\sqrt{3})$R30° structure of the sulfur headgroups. As a result, small domains of order and a high density of defects are observed in the film.

1. Introduction

The spontaneous formation of organized organic monolayers on solid surfaces continues to generate broad academic interest. Many studies have been motivated by the potential technological applications of self-assembled monolayers (SAMs). Monolayers of *n*-alkanethiols on Au(111) are the most thoroughly studied SAMs to date, and these systems are now relatively well characterized.[1−4] In recent years, the structural diversity of organic molecules investigated for SAM formation has expanded significantly. In particular, aromatic thiol SAMs have received attention due to their high electronic conductivity and nonlinear optical properties.[5−11] A number of studies have been carried out to deduce the structure and kinetics of film formation of aromatic thiols. It has been demonstrated that new packing structures may form when the relatively flexible hydrocarbon chain of the conventional alkanethiol SAM is replaced by a rigid and bulky aromatic moiety.[12−20] The nature of the intermolecular forces has been significantly modified: the dispersion forces responsible for chain ordering in alkanethiols have been augmented by anisotropic noncovalent $\pi-\pi$ and $\pi-\sigma$ interactions.[21]

For molecules containing only a single phenyl unit, such as benzenethiol on Au(111), consensus on the detailed structure of the SAMs has not yet been achieved. Well-ordered monolayers, with either an upright or strongly inclined adsorption geometry, or poorly organized films have been found after immersing Au(111) surfaces into benzenethiol.[14,19,20,22,23] This structural variation could arise from the different sample preparation conditions and may indicate that the interactions between single phenyl rings are only marginally strong enough to order commensurate films.

In addition to studies on thiols containing a single phenyl unit, oligophenylthiols have been studied. The pioneering work done by Sabatani et al. showed that 4-mercaptobiphenyl and 4-mecaptoterphenyl can form stable, ordered monolayers with similar surface concentrations to conventional alkanethiols.[24] They predicted a hexagonal packing structure on the basis of bulk crystal structures for these films. Other investigations include 4′-substituted biphenylthiols,[6,12,17,25] biphenyl-4-yl alkanethiols,[26] *p*-terphenyl derivatized thiols,[9,11,14] and oligo(phenylethynyl)benzenethiol[8,10,18,19] adsorbed on gold surfaces. For phenyl-substituted alkanethiols, the stability of the corresponding SAMs depends on the location of the benzene ring in the alkyl chain, as well as on the length of the chain.[15] With methylene "spacers" inserted between the biphenyl rings and the thiol headgroup, closely packed and ordered biphenyl-derivatized monolayers were formed.[15,26] When the thiol headgroup is directly connected with the oligophenyl rings, such as in 4′-substituted biphenylthiols, both incommensurate and hexagonal close-packed structures were reported.[12,17] Conjugated arenethiols, such as 4-[4′-(phenyl ethynyl)-phenylethynyl]benzenethiol, form ordered and incommensurate SAMs on gold surfaces.[18,19]

This paper describes a molecular scale investigation of methyl-terminated *p*-terphenyl thiol monolayers adsorbed on Au(111). The purpose is to achieve a better understanding of the intermolecular interactions and their effect on the stability and morphology of the films. Such a study is essential in understanding the electronic and optical properties of materials and devices based on oligophenyls. The monolayer thickness and the molecular orientation were determined by ellipsometry and reflection−absorption infrared spectroscopy (RAIRS). Film morphologies were characterized by scanning tunneling microscopy (STM).

2. Experimental Section

Synthesis. The preparation of *p*-methylterphenyl mercaptan was carried out according to the route shown in Scheme 1. *p*-Methylbiphenyl bromide (**1**) was prepared using published procedures.[27] The (*p*-methylterphenyl)methyl sulfide (**3**) was synthesized using Suzuki coupling[28] using approximately 0.5 g of **1** refluxed with 0.34 g of 4-(methylthio)phenylboronic acid (**2**) in the presence of 5 mol % of $Pd(PPh_3)_4$, 3.18 g of Na_2CO_3, 15 mL of H_2O and 40 mL of toluene under argon for 2 days. The resulting solution was extracted with CH_2Cl_2, dried

* Corresponding author. E-mail: garrett@cem.msu.edu. Phone: (517) 355-9715, ext. 208. Fax: (517) 353-1793.

10.1021/jp012123r CCC: $20.00
Published on Web 08/31/2001

SCHEME 1: Synthetic Scheme for MTPT Molecule[a,b]

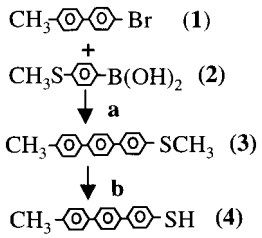

[a] 5 mol % $Pd(PPh_3)_4$, 3.18 g of Na_2CO_3, 15 mL of H_2O and 40 mL of Toluene, 48 h in Ar. [b] 5 equiv of $NaSCH_3$ in NMP, 100 °C, 48 h in N_2.

over Na_2SO_4, filtered through silica gel and concentrated to yield crude **3**. The crude product was recrystallized from CH_2Cl_2 to give a white solid. ^{13}C NMR and mass spectrometry were used to verify the structure and purity of **3**. The *p*-methylterphenyl thiol (MTPT) (**4**) was prepared by reaction of **3** and sodium thiomethoxide (5 equiv) in 1-methyl-pyrrolidin-2-one (NMP) under nitrogen.[29] The reaction ran at 100 °C for 2 days, and the solution was then extracted with ether and filtered through silica gel using CH_2Cl_2 as the eluting solvent. The light-yellow solution of **4** was then concentrated until saturation (~1 mM). Mass spectra of the solution give the appropriate molecular peak at mw 276.

Substrate and Monolayer Preparation. The gold substrates for infrared spectroscopy and ellipsometry measurements were made by electron-beam evaporation of 200 nm of Au on 20 nm of Ti on Si(100) wafers. The gold substrates for STM measurements were prepared by thermally evaporating gold onto freshly cleaved mica in high vacuum. In both cases, STM revealed the clean surfaces to be composed of Au grains with (111)-textured terraces (1000−2500 Å) separated by monatomic steps. All of the substrates were cleaned by a UV/O_3 cleaner for 15 min, followed by soaking in deionized water for 30 min. After this, the substrates were dried in flowing N_2 and immediately transferred into a saturated solution of MTPT in CH_2Cl_2 for 3−18 h, followed by rinsing with copious quantities of CH_2Cl_2 and drying in a N_2(g) stream.

Surface Characterization. Reflection−absorption infrared spectroscopy was performed using a N_2-purged Nicolet 560 Magna IR spectrometer with MCT detector. Spectra were obtained with a PIKE specular reflectance accessory using *p*-polarized light incident at 80° with respect to the normal surface. All spectra reported were the average of 256 scans obtained at a resolution of 4 cm^{-1} and referenced to a freshly prepared, clean gold film. Transmission spectra of the pure compounds were recorded on a Mattson 3000 Galaxy Series Fourier transform infrared (FTIR) spectrometer. Film thickness was determined by using a rotating analyzer ellipsometer with a white light source and an incidence angle of 75° with respect to the surface normal. Forty-four wavelengths between 414 and 736 nm were used to fit the ellipsometric data, and at least six sampling areas were used to obtain an average film thickness. All STM images were obtained in UHV ($<1 \times 10^{-9}$ Torr) using a RHK Technology model UHV-300 scanning tunneling microscope. The STM tips were mechanically cut $Pt_{0.8}Ir_{0.2}$ wires. Typical tunneling currents were 10−100 pA, and a bias voltage of +300 mV was applied to the sample.

3. Results and Discussion

Self-assembled monolayers of MTPT on Au(111) were initially characterized by ellipsometric and RAIRS measurements. Ellipsometry showed that the average film thickness was 17 ± 1 Å, indicating the presence of a densely packed monolayer with the molecular axes slightly tilted away from the surface normal. The length of one MTPT molecule was calculated to be 15.4 Å,[30] and on the basis of the S−Au distance of 2.36 Å,[8] a tilt angle of 17 ± 8° was determined. Similar results were also observed for other terphenyl thiol derivatized SAMs on gold, with tilt angles ranging from 5° to 27° reported.[11,14,24]

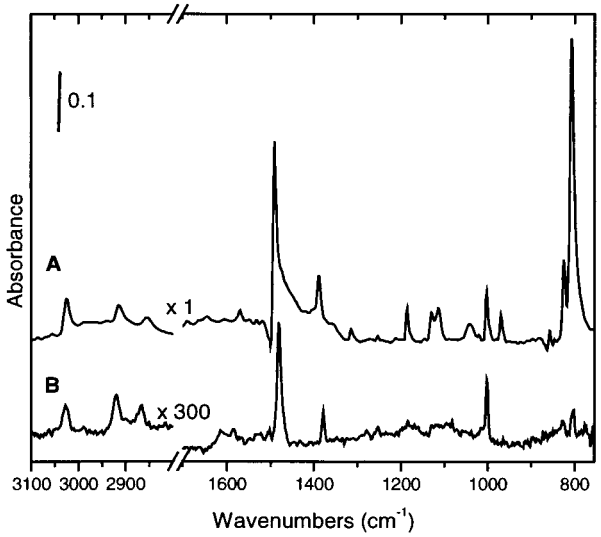

Figure 1. IR spectra of (A) DMTP solid in KBr pellet and (B) MTPT monolayer on a Au/Si wafer.

Reflection−absorption infrared spectroscopy confirmed the adsorption of MTPT on gold. Comparison of the reflectance spectrum of the MTPT SAM with the transmission spectrum of 4,4″-dimethyl terphenyl (DMTP)[31] solid in KBr supported the conclusion that the molecular axes in the SAM were nearly perpendicular to the substrate surface plane. Because of the limited quantities of MTPT generated, DMTP was chosen for RAIRS comparison because of the structural similarity to the MTPT molecule. Variation in para substituents may affect band positions and intensities;[32] however, changing the 4-substituent from methyl (in DMTP) to thiol (in MTPT) should not alter the charge distribution in the aromatic ring significantly because thiol is a weak electron donor.[33] Therefore, we believe the IR spectrum of MTPT solid will be similar to that of the DMTP solid, and it is valid to compare MTPT SAM RAIRS data with DMTP transmission data in order to obtain orientational information in the monolayer.

Figure 1A shows the transmission spectrum of DMTP solid in KBr, and Figure 1B shows the RAIR spectra of MTPT SAM on Au(111). All peaks in these spectra can be assigned by consulting the data in the literature,[12,26,33−35] and the results are summarized in Table 1. The DMTP bulk spectrum is dominated by two aromatic vibrations: the ring C−C stretch (1490 cm^{-1}, 19a) and the out-of-plane C−H bend (808 cm^{-1}, 17b), whose transition dipoles are oriented parallel to the 4,4″ axis and orthogonal to the ring plane of the terphenyl moiety, respectively. Four aromatic C−H in-plane deformation bands occur in the region 1187−970 cm^{-1} in the DMTP bulk spectrum, and among these bands, only mode 18a at 1003 cm^{-1} has its dynamic dipole aligned parallel to the 4,4″ axis. In the range of aromatic C−H stretching modes, only one strong band shows up at 3025 cm^{-1} (20b). The terminal CH_3 has two prominent bands at 2914 and 2856 cm^{-1}, both assigned to symmetric CH_3 stretches. The asymmetric CH_3 stretching vibrations are not degenerate and are seen as two weak bands at 2974 and 2940 cm^{-1}. The asymmetric and symmetric CH_3 bending vibrations are located at 1466 and 1389 cm^{-1}, respectively, with the first

TABLE 1: Infrared Band Assignments for MTPT SAM and DMTP Solid in KBr[a]

peak position (cm^{-1})			
solid DMTP in KBr	MTPT SAM	mode assignment	direction of transition dipole[b]
3026	3029	νCH_{arom} (20b)[b]	$\perp$ 4,4″ axis, ip
2974	−	$\nu_{as}CH_3$	$\perp$ 4,4″ axis
2940	−	$\nu_{as}CH_3$	$\perp$ 4,4″ axis
2914	2920	ν_sCH_3	$\parallel$ 4,4″ axis
2856	2865	ν_sCH_3	$\parallel$ 4,4″ axis
1490	1481	νCC_{arom} (19a)[c]	$\parallel$ 4,4″ axis
1466(sh)	−	$\delta_{as}CH_3$	$\perp$ 4,4″ axis
1388	1379	δ_sCH_3	$\parallel$ 4,4″ axis
1187	−	δCH_{arom}	$\perp$ 4,4″ axis
1115	−	δCH_{arom}	$\perp$ 4,4″ axis
1041	−	$\delta_{as}CH_3$	$\perp$ 4,4″ axis
1003	1002	δCH_{arom} (18a)[c]	$\parallel$ 4,4″ axis
970	−	δCH_{arom}	$\perp$ 4,4″ axis
825	826	νCC_{arom} (1)[c]	$\perp$ 4,4″ axis, op
808	806	ωCH_{arom} (17b)[c]	$\perp$ 4,4″ axis, op

[a] −, not observed; sh, shoulder; op, out-of-plane; ν, stretching vibration; δ, in-plane bending vibration; ω, out-of-plane bending vibration. [b] Based on C_s symmetry. [c] Wilson's notation.

band strongly overlapped by the aromatic ring stretch. The CH_3 rock vibration appears as a weak band at 1040 cm^{-1}.

The RAIR spectrum of MTPT SAM looks much simpler than the bulk DMTP spectrum. The simplification of the spectrum in the SAM environment reflects the nearly perpendicular orientation of the terphenyl moiety to the substrate surface. Most striking is the intensity drop of the aromatic out-of-plane bending mode at 806 cm^{-1} (17b). In contrast to the out-of-plane vibration, the ring C−C stretching mode (1481 cm^{-1}, 19a) and in-plane C−H bending mode (1003 cm^{-1}, 18a), whose transition dipoles are parallel to the 4,4″ axis, have significant intensity. According to the infrared surface selection rule, only vibrations with transition dipole moments oriented perpendicular to the metal substrate are observed. Therefore, peak intensities are directly related to the component of each transition moment that is perpendicular to the metal surface. It should be noted that changes in the intrinsic oscillator strength, for example, by a perturbation of the vibrational potential energy surface induced by changes in layer packing, will also affect the intensity of an IR absorption band. This effect is ignored in the present discussion. The dramatic diminution of mode 17b and the strong absorption of modes 19a and 18a suggest that the aromatic rings in the film are roughly perpendicular to the plane of the gold surface. Similar conclusions were derived in the RAIRS data of other oligophenylthiol SAMs.[12,21,26]

The small molecular tilt argument is also supported by intensity changes in the CH_3 vibrational modes. Both symmetric stretching (2920 and 2865 cm^{-1}) and in-plane bending (1379 cm^{-1}) modes, whose transition dipoles are parallel to the 4,4″ axis, appear distinctively in the spectrum of MTPT SAM, whereas the asymmetric stretching and in-plane bending modes were absent.

A typical large area STM image of the MTPT monolayer on Au(111) after >10 h soaking is shown in Figure 2. The image shows three terraces separated by monatomic height steps in the Au substrate. Also visible are small, irregularly shaped islands approximately 50−150 Å in diameter distributed on the terraces. The islands do not appear to be correlated with the position of step edges in the substrate. The height of the individual islands was measured as 2.6 ± 0.3 Å, consistent with the height of a single atomic layer of Au (measured in our instrument as 2.5 ± 0.2 Å).[36]

Compared with aliphatic thiol[4,37] or aliphatic/aromatic mixed thiol[38] SAMs, the presence of islands rather than depressions in the monolayer is rather surprising. Conventional *n*-alkanethiols typically produce monatomic deep depressions in the monolayer (termed "vacancy islands").[39] The vacancy islands form during the adsorption process of alkanethiols on Au(111), and at high surface coverage, the $(\sqrt{3}\times\sqrt{3})R30°$ lattice structure is observed within the depressions.[40] The origin of vacancy islands is still controversial but appears to be related to lifting of the $23\times\sqrt{3}$ compressed herringbone reconstruction of the bare Au surface, followed by expulsion of additional atoms from the relaxed surface.[39]

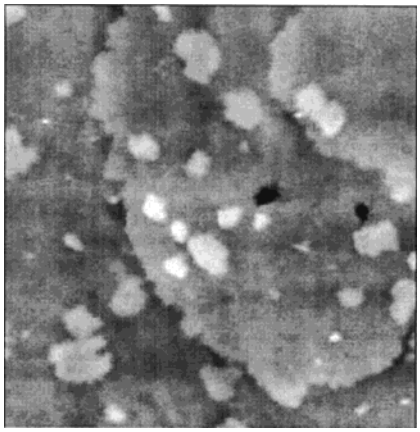

Figure 2. Large-scale STM image of MTPT on Au(111). Three terraces separated by monatomic steps are shown. Islands with a height of 2.6 ± 0.3 Å are observed. Image size: 1500 × 1500 Å.

Under our monolayer preparation conditions, the islands appeared to be stable for at least several hours without observable changes in size, shape, or structure (we have observed very rapid self-diffusion of gold atoms on Au(111) surfaces under the same time scale). In addition, we obtained identical molecular resolution images both on top of the islands and on the surrounding terraces, suggesting that the islands were not associated with different structural phases but, rather, formed in a homogeneous layer. Similar island structures were also observed on other aromatic thiol SAMs.[13] Upon adsorption of 4-mercaptopyridine (4MPY) or 4-hydroxythiophenol (4HTP) molecules on Au(111), monatomic high islands appeared immediately on the gold terraces. The islands initially increased both in size and number, and then decreased slowly after reaching maximum values (the coverage of the islands reached 50% in 15 min). The formation of the islands was attributed to gold atoms on the surface which became highly mobile due to strong binding to the thiols. It was suggested that islands are formed on aromatic thiols rather than depressions because the strong attractive intermolecular interactions between the phenyl moieties favors aggregation of the adsorbed aromatic molecules (each with a gold atom attached) into islands. Although we were not able to observe the formation of the islands on flat Au(111) regions by STM (for example, during the adsorption process), on the basis of the dimensions, density, and surface coverage of the islands, we believe the monatomic high islands on our MTPT SAMs were probably formed in the same manner as those in 4MPY and 4HTP SAMs during the initial adsorption under conditions of high Au mobility.

On the terraces, we were able to observe the molecular arrangement of MTPT molecules on Au(111). Figure 3A shows a typical high resolution STM image of the MTPT monolayer on a single Au(111) terrace. Molecules appeared as single circular or oval features arranged in a hexagonal pattern, and this same packing was consistently observed on the terraces and the monatomic high islands. Close inspection of MTPT SAM revealed that there were many defects and disordered

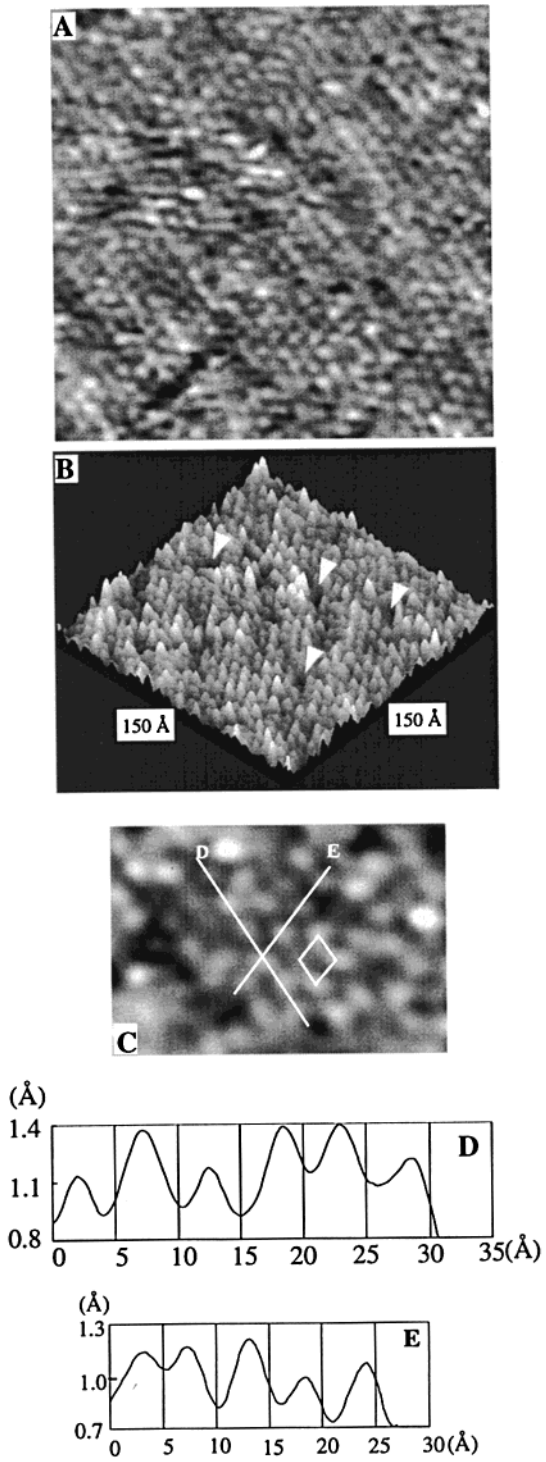

Figure 3. High-resolution STM images of MTPT monolayer on Au(111). Image size: (A and B) 150 × 150 Å; (C) 40 × 60 Å. Panels D and E show the corresponding line profiles in panel C.

regions in the monolayer (some are pointed out in Figure 3B). Although rows of molecules can be observed easily, the degree of order is significantly less than that of a typical alkanethiol SAM. The image appears to be composed of many small regions of order (approximately 30−60 Å in diameter containing about 25−100 molecules) surrounded by disorder and defects. The origin of the defects will be discussed below.

A similar hexagonal packing structure was also reported for 4-methyl-4′-mercaptobiphenyl (MMB) SAM on Au(111), as characterized by grazing incidence X-ray diffraction (GIXD) and low-energy atomic beam diffraction (LEAD).[17] The MMB

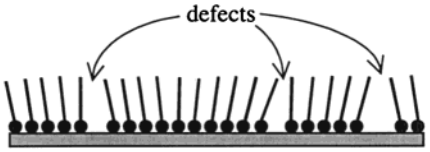

Figure 4. Model showing the adsorbed sulfur atoms as black circles and the molecular chains as lines along the molecular axis. The sulfur atoms are separated by 5.0 Å as in a $(\sqrt{3}\times\sqrt{3})$R30° structure, while the ω terminus of the aromatic portion of the molecules are separated by 5.3 Å.

molecule has one less phenyl ring than the MTPT molecule of our study but has the same α and ω substituents. In addition to the high-density hexagonal phase, a low-density striped phase was also observed following gas-phase deposition. After conventional liquid-phase deposition, no phase other than the hexagonal phase was seen, and on the basis of the diffraction peak widths, the domain size was estimated to be ∼65 Å. Clearly, our STM data for the terphenyl SAM supports the conclusions of Leung et al. for the biphenyl system.[17] These aromatic SAMs appear to be composed of small domains of ordered material when deposition is carried out in solution.

In small ordered domains as shown in Figure 3C, the measured lattice vectors were $a = 5.3 \pm 0.3$ Å, $b = 5.3 \pm 0.4$ Å, and $\gamma = 60 \pm 2°$. These values were calculated from at least 20 different domains, and typical cross-section data are presented in Figure 3D,E. While generally consistent with the $(\sqrt{3}\times\sqrt{3})$R30° structure observed for many alkanethiols ($a = b = 4.99$ Å, $\gamma = 60°$), the MTPT primitive unit cell is ∼11% larger in area. Indeed, calibration experiments on octanethiol SAMs were performed under identical conditions and produced lattice vectors of $a = b = 5.0 \pm 0.2$ Å. An examination of the molecular crystal of terphenyl[41] shows that the area per molecule in the (001) plane of the crystal is about 6% larger than that of the molecule in the $(\sqrt{3}\times\sqrt{3})$R30° lattice.[24] It appears from our STM images that commensurate monolayers of MTPT cannot be formed with long-range two-dimensional order. Instead, local $(\sqrt{3}\times\sqrt{3})$R30° Au−S bonding probably occurs; however, the aryl part of the molecule attempts to adopt the larger separation dictated by $\pi-\pi$/van der Waals interactions as in the molecular crystal. The MTPT molecules may accommodate the strain by tilting of the molecular axis (and likely some twisting). This tilt most likely increases progressively with distance from the center of the ordered area, but eventually restricts $(\sqrt{3}\times\sqrt{3})$R30°-like Au−S bonding, as shown schematically in Figure 4. Such a situation would account for the small areas of order surrounded by disorder observed in our STM images.

In the biphenyl-based MMB monolayer, GIXD results showed that the underlying sulfur atoms were in an ordered $(\sqrt{3}\times\sqrt{3})$-R30°-like structure.[17] However, some surface disorder was detected by LEAD, a technique that is only sensitive to the position of the topmost layer of atoms. This disorder was attributed to mismatch between the lowest-energy configuration of the biphenyl backbone and that of the underlying $(\sqrt{3}\times\sqrt{3})$-R30° structure of the sulfur headgroups. Small ordered domains and high defect density were also reported in other aromatic thiol SAMs.[12,18,19]

For 4-[4′(phenylethynyl)-phenylethynyl]-benzenthiol and 4′-chloro-4-mercaptobiphenyl SAMs,[12,18] an ordered but incommensurate structure has been reported. In both monolayers, six equivalent domains were present, and superstructures were observed. A rectangular unit cell containing two molecules was revealed in STM images and was similar to the bulk terphenyl crystal structure. Compared with these monolayers, our MTPT SAMs did not show evidence of large dimensional superstruc-

tures or periodic Moire fringes. Our unit cells were hexagonal and exhibited the three rotational domains characteristic of a commensurate lattice. The precise cause of the structural differences between MTPT and 4-[4′(phenylethynyl)-phenylethynyl]-benzenthiol or 4′-chloro-4-mercaptobiphenyl monolayers may be related to steric factors or electronic effects due to different ω substitution. It has been already demonstrated that different ω position substituents on the aromatic ring can affect the molecular structure of the self-assembled films significantly.[11,15]

We annealed the MTPT monolayers in UHV at 45 °C for 30 min to investigate whether "lying-down" phases, as observed for octadecanethiol ($C_{18}H_{37}SH$), could be generated. Octadecanethiol, which has a similar mass and number of carbon atoms as MTPT, exhibited a variety of $p\times\sqrt{3}$ monolayer structures after 30 min of annealing at 45 °C.[42] However, STM revealed that the MTPT monolayer had completely desorbed after annealing: we found no evidence for the intermediate $p\times\sqrt{3}$ phases. This clearly suggests that the overall intermolecular interchain interactions are weaker in aromatic versus aliphatic thiols. Unfortunately, we cannot independently assess the role of the domain size in the thermal stability, although we might expect the small domain/moderately disordered terphenyl thiol SAMs to exhibit reduced thermal stability compared with the large domain/fully ordered alkanethiol SAMs.

4. Conclusions

Self-assembled monolayers (SAMs) of rigid *p*-methylterphenyl thiol (MTPT) on Au(111) were investigated by ellipsometry, RAIRS, and STM. The aromatic nature and rigidity of the molecular backbone influenced the final monolayer structure, and different film properties were observed compared with conventional alkanethiol SAMs. According to ellipsometry and RAIRS, MTPT formed densely packed monolayers on gold with the molecular axes slightly tilted away from the surface normal (~17°). At room temperature, monatomically high islands were observed by STM instead of the typical monatomically deep holes in alkanethiol SAMs. Molecular resolution images of the MTPT monolayer revealed a $(\sqrt{3}\times\sqrt{3})$R30°-like packing with slightly larger lattice vectors than those of typical alkanethiol monolayers.

Several energetic interactions contribute to the self-assembly and stabilization of alkane and substituted alkanethiol monolayers on Au(111). These include the covalent S−Au bonding, van der Waals' chain−chain interactions, and end group-end group interactions. In general, when S−Au bonding is dominant, the usual $(\sqrt{3}\times\sqrt{3})$R30° packing results. However, in aromatic thiols, there are additional intermolecular forces derived from the π systems of neighbors,[43] and it is possible to form new room-temperature monolayer phases. When interchain interactions are dominant, an ordered but incommensurate layer may be formed as observed for 4-[4′ (phenylethynyl)-phenylethynyl]-benzenthiol and 4′-chloro-4-mercaptobiphenyl monolayers.[12,18] In the present system, the interchain $\pi-\pi$ and S−Au interactions appear to be of similar magnitude. The result is that small domains of $(\sqrt{3}\times\sqrt{3})$R30°-like packing were observed by STM, but the structural restrictions imposed by the terphenyl portion of the MTPT create strain in the domain. This inhibits the formation of long-range two-dimensional order.

Acknowledgment. This work was partly supported by the Center for Fundamental Materials Research (CFMR) at Michigan State University. We gratefully acknowledge Prof. G. L. Baker and Tianqi Liu for assistance with the synthesis of the MTPM molecule.

References and Notes

(1) Ulman, A. *An Introduction to Ultrathin Organic Films: From Langmuir−Blodgett to Self-Assembly*; Academic Press: Boston, 1991.
(2) Ulman, A. *Chem. Rev.* **1996**, *96*, 1533.
(3) Poirier, G. E. *Chem. Rev.* **1997**, *97*, 1117.
(4) Poirier, G. E.; Fitts, W. P.; White, J. M. *Langmuir* **2001**, *17*, 1176.
(5) Buckel, F.; Effenberger, F.; Yan, C.; Gölzhäuser, A.; Grunze, M. *Adv. Mater.* **2000**, *12*, 901.
(6) Kang, J. F.; Ulman, A.; Jordan, R.; Kurth, D. G. *Langmuir* **1999**, *15*, 5555.
(7) Eck, W.; Stadler, V.; Geyer, W.; Zharnicov, M.; Gölzhäuser, A.; Grunze, M. *Adv. Mater.* **2000**, *12*, 805.
(8) Tour, J. M.; Jones, L., II; Pearson, D. L.; Lamba, J. J. S.; Burgin, T. P.; Whitesides, G. M.; Allara, D. L.; Parkh, A. N.; Atre, S. V. *J. Am. Chem. Soc.* **1995**, *117*, 9529.
(9) Ishida, T.; Mizutani, W.; Akiba, U.; Umemura, K.; Inoue, A.; Choi, N.; Fujihira, M.; Tokumoto, H. *J. Phys. Chem. B* **1999**, *103*, 1686.
(10) Zehner, R. W.; Sita, L. R. *Langmuir* **1997**, *13*, 2973.
(11) Himmel, H.-J.; Terfort, A.; Wöll, C. *J. Am. Chem. Soc.* **1998**, *120*, 12069.
(12) Kang, J. F.; Ulman, A.; Liao, S.; Jordan, R.; Yang, G.; Liu, G.-Y. *Langmuir* **2001**, *17*, 95.
(13) Jin, Q.; Rodriguez, J. A.; Li, C. Z.; Darici, Y.; Tao, N. J. *Surf. Sci.* **1999**, *425*, 101.
(14) Frey, S.; Stadler, V.; Heister, K.; Eck, W.; Zharnikov, M.; Grunze, M.; Zeysing, B.; Terfort, A. *Langmuir* **2001**, *17*, 2408.
(15) Tao, Y.-T.; Wu, C.-C.; Eu, J.-Y.; Lin, W.-L. *Langmuir* **1997**, *13*, 4018.
(16) Ulman, A.; Scaringe, R. P. *Langmuir* **1992**, *8*, 894.
(17) Leung, T. Y. B.; Schwartz, P.; Scoles, G.; Schreiber, F.; Ulman, A. *Surf. Sci.* **2000**, *458*, 34.
(18) Yang, G.; Qian, Y.; Engtrakul, C.; Sita, L. R.; Liu, G.-Y. *J. Phys. Chem. B* **2000**, *104*, 9059.
(19) Dhirani, A.; Zehner, R. W.; Hsung, R. P.; Guyot-Sionnest, P.; Sita, L. R. *J. Am. Chem. Soc.* **1996**, *118*, 3319.
(20) Wan, L. J.; Terashima, M.; Noda, H.; Osawa, M. *J. Phys. Chem. B* **2000**, *104*, 3563.
(21) Reese, S.; Fox, M. A. *J. Phys. Chem. B* **1998**, *102*, 9820.
(22) Szafranski, C. A.; Tanner, W.; Laibinis, P. E.; Garrell, R. L. *Langmuir* **1998**, *14*, 3570.
(23) Whelan, C. M.; Smyth, M. R.; Barnes, C. J. *Langmuir* **1999**, *15*, 116.
(24) Sabatani, E.; Cohen-Boulakia, J.; Bruening, M.; Rubinstein, I. *Langmuir* **1993**, *9*, 2974.
(25) Kang, J. F.; Ulman, A.; Liao, S.; Jordan, R. *Langmuir* **1999**, *15*, 2095.
(26) Rong, H.-T.; Frey, S.; Yang, Y.-J.; Zharnikov, M.; Buck, M.; Wühn, M.; Wöll, C.; Helmchen, G. *Langmuir* **2001**, *17*, 1582.
(27) Bumagin, N. A.; Luzikova, E. V.; Beletskaya, I. P. *Russ. J. Org. Chem.* **1995**, *31*, 1480.
(28) Miyaura, N.; Yanagi, T.; Suzuki, A. *Synth. Commun.* **1981**, *11*, 513.
(29) Shaw, J. *J. Org. Chem.* **1991**, *56*, 3728.
(30) Molecular mechanics calculations were performed by using the SPARTAN 5.0 molecular modeling program (Wavefunction Inc., CA), based on empirical Merck force fields.
(31) DMTP was synthesised using Suzuki coupling of *para*-methylbiphenyl bromide and 4-methylphenylboronic acid.
(32) Avram, M.; Mateescu, G. D. *Infrared Spectroscopy: Applications in Organic Chemistry*; Wiley-Interscience: New York, 1966.
(33) Colthup, N. B.; Daly, L. H.; Wiberley, S. E. *Introduction to Infrared and Raman Spectroscopy*; Academic Press: Boston, 1990.
(34) Varsanyi, G. *Vibrational Spectra of Benzene Derivatives*; Academic Press: New York, 1969.
(35) Varsanyi, G. *Assignments for Vibrational Spectra of Seven Hundred Benzene Derivatives*; John Wiley and Sons: New York, 1974; Vol. 1.
(36) Poirier, G. E.; Tarlov, M. J. *J. Phys. Chem.* **1995**, *99*, 10966−10970.
(37) Poirier, G. E.; Pylant, E. D. *Science* **1996**, *272*, 1145.
(38) Duan, L.; Garrett, S. J. *Langmuir* **2001**, *17*, 2986.
(39) Poirier, G. E. *Langmuir* **1997**, *13*, 2019.
(40) Schönenberger, C.; Sondag-Huethorst, J. A. M.; Jorritsma, J.; Fokkink, L. G. *Langmuir* **1994**, *10*, 611.
(41) Rietveld, H. M.; Maslen, E. N.; Clews, C. J. B. *Acta Crystallogr., Sect. B* **1970**, *26*, 693.
(42) Duan, L.; Garrett, S. J. Unpublished results, 1998.
(43) Lii, J.-H.; Allinger, N. L. *J. Am. Chem. Soc.* **1989**, *111*, 8576.